THE MODE MATCHING METHOD APPLIED TO BEAM COUPLING IMPEDANCE CALCULATIONS OF FINITE LENGTH DEVICES

N. Biancacci, CERN, Geneva, Switzerland; Rome University "La Sapienza", Rome, Italy
V.G.Vaccaro, CERN, Geneva, Switzerland; University Federico II, Naples, Italy
E.Metral, B.Salvant, CERN, Geneva, Switzerland
M.Migliorati, L.Palumbo, Rome University "La Sapienza", Rome, Italy

Abstract

The infinite length approximation is often used to simplify the calculation of the beam coupling impedance of accelerator elements. This is expected to be a reasonable assumption for devices whose length is greater than the transverse dimension but may be less accurate approximation for segmented devices. In this contribution we present the study of the beam coupling impedance of a finite length device: a cylindrical cavity loaded with a toroidal slab of lossy dielectric. In order to take into account the finite length, we will decompose the fields in the cavity and in the beam pipe into a set of orthonormal modes and apply the mode matching method to obtain the impedance. To validate our method, we will present comparisons between analytical formulas and 3D electromagnetic CST simulations as well as applications to the evaluation of the impedance of short beam pipe inserts, where the longitudinal and transverse dimensions are difficult to model in numerical simulations.

INTRODUCTION

The problem of calculating the impedance of finite length devices, in particular simple cavities as shown in Figure 1, has been approached in different ways: it was studied as a field matching problem in [1], and, approximated as a thin insert in [2,3].

In this application we want to study rigorously the electromagnetic fields by means of the mode matching method [4, 5].

DESCRIPTION OF THE METHOD

The structure we studied is shown in Figure 1: the regions I and II represent the cylindrical left and right beam pipes where the reflected fields will propagate ($z \in (-\infty, 0) \cup (L, +\infty), r \in (0, b)$), region III is the cavity where resonances can be excited ($z \in (0, L), r \in (0, b)$) and region IV is the toroidal insert ($z \in (0, L), r \in (b, c)$) where radial waves can propagate.

The beam $\rho_z(r, z; \omega)$ is represented in frequency domain as a thin ring of radius a and charge Q:

$$\rho_z(r, z; \omega) = \frac{Q}{2\pi a}\delta(r - a)e^{-jk_0 z}, \quad (1)$$

where $k_0 = \omega/\beta c$ is the propagation constant of the beam.

In order to handle the problem of determining the longitudinal beam coupling impedance, the electromagnetic field induced by the source will be calculated as a superposition of an impressed and a scattered field:

$$\bar{E}^{(tot)} = \bar{E}^{(source)} + \bar{E}^{(scattered)}$$

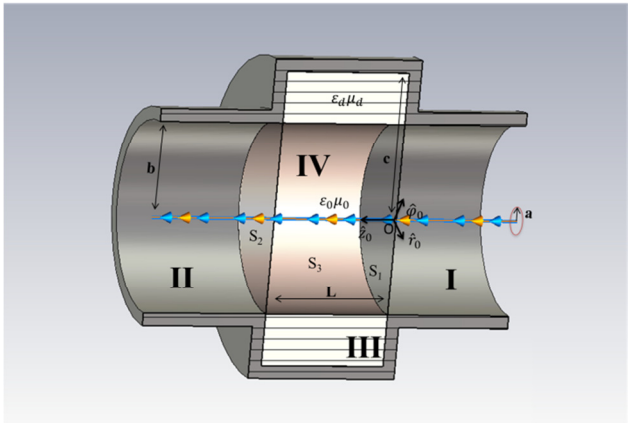

Figure 1: Model studied with the mode matching method.

The primary field and the scattered field in all the four regions consist in Transverse Magnetic waves: all the components can be derived by the longitudinal electric field E_z .

Source Fields

The source field $\bar{E}^{(source)}$ is calculated as the field induced by the source particle travelling at speed βc, i.e. representing a current $J_z = \rho_z \beta c$, along the axis of the perfectly conducting (PEC) beam pipe of radius b. This field is given by the following formula,

$$E_z^{(source)} = \frac{j\alpha_b Q\, Z_0}{2\pi\gamma^2\beta b}\left[K_0(u) - \frac{K_0(x)}{I_0(x)}I_0(u)\right]e^{-jk_0 z}, \quad (2)$$

where $Z_0 = 376.73\Omega$ the characteristic impedance of vacuum, K_0, I_0 the modified Bessel functions of argument $x = k_0 b/\gamma$ and $u = k_0\, r$.

Scattered field

In region I we have the following expression for the longitudinal electric field [4, 5]:

$$E_z^{(left)} = \sum_p^{\infty} \boldsymbol{C_p}\frac{J_0(\alpha_p r/b)}{b\sqrt{\pi}J_1(\alpha_p)}e^{j\tilde{\alpha}_p z/b}. \quad (3)$$

In region II we have

ISBN 978-3-95450-115-1

$$E_z^{(right)} = \sum_p \boldsymbol{D_p} \frac{J_0(\alpha_p r/b)}{b\sqrt{\pi} J_1(\alpha_p)} e^{-j\tilde{\alpha}_p (z-L)/b}, \quad (4)$$

where α_p, with $p \in \mathrm{N}$, are the zeros of the Bessel function $J_0(r)$, $\tilde{\alpha}_p = \sqrt{\alpha_0^2 - \alpha_p^2}$, $\alpha_0 = k_0 b = \omega\sqrt{\mu_0 \varepsilon_0}\, b$, $\alpha_1 = 2.405$.

In region IV:

$$E_z^{(rad)} = \sum_s \boldsymbol{A_s} W_s(\hat{\alpha}_s r/b) cos(\alpha_s z/b), \quad (5)$$

where the function $W_s(\tilde{\alpha}_s r/b)$ describe the radial waves as [4, 5]:

$$W_s(\hat{\alpha}_s/b) = H_0^{(2)}\left(\frac{\hat{\alpha}_s r}{b}\right) - \frac{H_0^{(2)}\left(\frac{\hat{\alpha}_s c}{b}\right)}{H_0^{(1)}\left(\frac{\hat{\alpha}_s c}{b}\right)} H_0^{(1)}\left(\frac{\hat{\alpha}_s r}{b}\right),$$

with $\alpha_d = k_d b = \omega\sqrt{\mu_d \varepsilon_d}\, b$, $\alpha_s = s\pi b/L$, where d refers to the dielectric insert and $\hat{\alpha}_s = \sqrt{{\alpha_d}^2 - {\alpha_s}^2}$ and Z_d is the characteristic impedance in this region.

In region III we can expand the field in a complete set of orthonormal modes of TM type associated to homogeneous boundary condition on S_1, S_2 and S_3:

$$\bar{E}^{(cav)} = \sum_{ps} \boldsymbol{V_{ps}}\, \bar{e}_{ps}. \quad (6)$$

The longitudinal component of the electric field has the following expression:

$$E_z^{(cav)} = \sum_{ps}^{\infty} \boldsymbol{V_{ps}} \frac{\alpha_p}{\alpha_{ps}} \sqrt{\frac{\varepsilon_s}{L}} \frac{J_0\left(\frac{\alpha_p r}{b}\right)}{b\sqrt{\pi} J_1(\alpha_p)} cos\left(\frac{\alpha_s z}{b}\right), \quad (7)$$

where $\alpha_{ps} = \sqrt{\alpha_p^2 + \alpha_s^2}$. In summary four infinite vectors $\{\boldsymbol{V_{ps}}\}$, $\{\boldsymbol{A_s}\}$, $\{\boldsymbol{C_p}\}$ and $\{\boldsymbol{D_p}\}$ are the unknowns.

Matching Conditions

By matching the tangential components of the magnetic field on the boundary surfaces S_1, S_2, S_3, we obtain 3 functional equations. By means of an ad-hoc projection (Ritz-Galerkin method) each functional equation may be transformed into an infinite set of linear equations.

In order to get a fourth equation we should find a tool to match the tangential component of the electric field. This is not as simple as for the magnetic field since, according to the assumed expansion, the tangential component of the electric field on the boundary $S = S_1 \cup S_2 \cup S_3$ is null by definition. One has to note that in this case the expansion given by Eq. (7) will not converge uniformly on the boundaries. However, this difficulty may be circumvented by resorting to the following equation [4]

$$\boldsymbol{V_{ps}} = \frac{\alpha_0 b}{(\alpha_0^2 - \alpha_{ps}^2)} \oint_S \left(\bar{E} \times \bar{h}_{ps}^*\right) \cdot \hat{r}_0 dS. \quad (8)$$

An ad-hoc truncation is applied to the infinite set of the linear equations and then the four sets of equations are solved.

Once all the vectors are known, the coupling impedance can be easily calculated.

APPLICATIONS

A first series of benchmark was done with the standard theory and CST particle simulations [6].

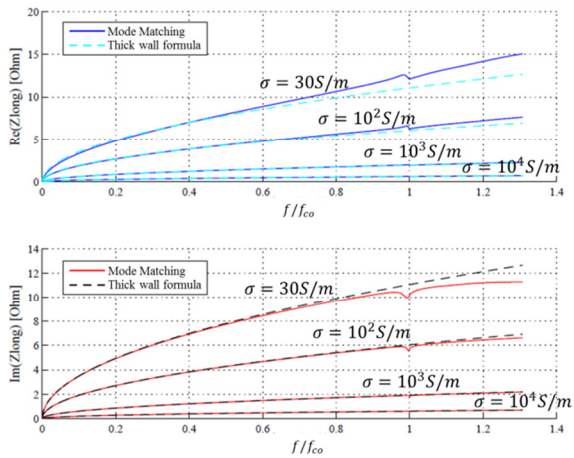

Figure 2: Comparison of the mode matching method (full lines) with the standard thick wall formula (dashed lines) for various conductivities and b=5cm, c=30cm, L=20cm; $\varepsilon_d = 8\varepsilon_0 - j\,\sigma/\omega$; $\mu_d = \mu_0$; $f_{co} = \alpha_1 c\,/2\pi b$.

In Figure 2 we show the comparison with the standard theory for thick wall [7]: the agreement is good for high conductivity, while it starts to be significantly different for low conductivity at frequencies above cut-off (f is normalized to the cut-off frequency f_{co}). In fact, with decreasing conductivity the insert surface impedance becomes more and more different from the surface impedance of the adjacent pipes I and II. This implies that the losses due to the scattered wave into the pipes, which can propagate only above cut-off, become comparable to those produced into the volume IV. As a conclusion, when a pipe exhibits a discontinuity in the surface impedance this discontinuity will contribute to increase the broad band impedance. This effect is not taken into account by the standard theory.

To complete the picture, in Figure 3 we study the same device for low conductivity: the skin depth becomes comparable with the transverse dimension of the cavity and the transverse field can "see" the cavity's boundary and be reflected giving rise to resonances. This sets a lower limit of conductivity for the classical thick wall formula validity.

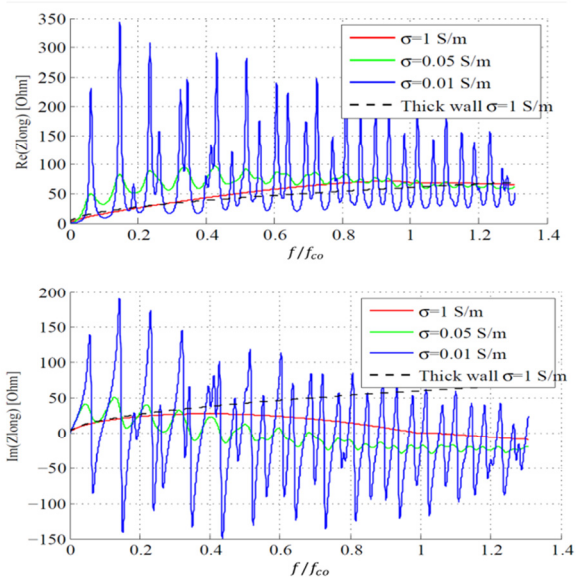

Figure 3: Application of the mode matching method for low values of conductivity.

In Figure 4 we show another comparison for a material with low conductivity ($\sigma \cong 10^{-2}\ S/m$): the cut-off between resonant modes and broadband behaviour is clearly visible. The discrepancy above cut-off is intrinsic to the CST solving tool.

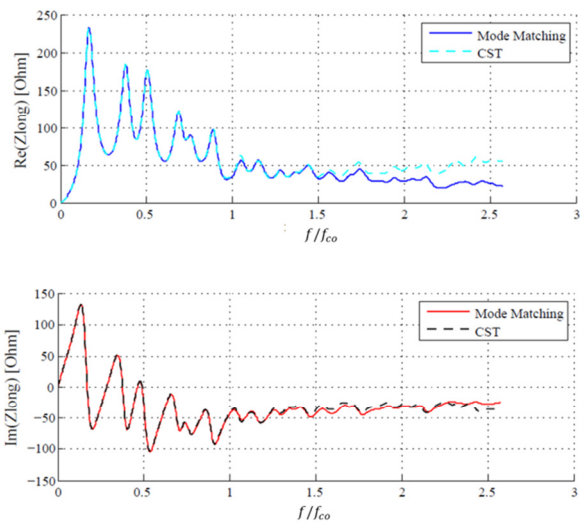

Figure 4: Comparison with CST simulations: b=5cm, c=30cm, L=20cm. Material: ε_{dr}=1, μ_{dr}=1, σ=10^{-2} S/m.

Another cross-check was done in order to study the SPS flanges impedance. A flange can be seen as a very short re-entrance between two beam pipes whose impedance cannot be easily studied with CST due to geometrical limitations (800 μm gap width with 5 cm beam pipe radius) and due to the very low dielectric losses that make the Q factor - and then the wake length - very large.

The comparison in Figure 5 shows only a partial agreement between mode matching and CST simulations with some discrepancy for the peak below cut-off (left plot). The peak mismatch is due to the fact that the wake in CST has not completely decayed: in this case the number of mesh cells (10^6) was a limitation (we took a rms bunch length of 1.5cm and a maximum wake length of 20 m).

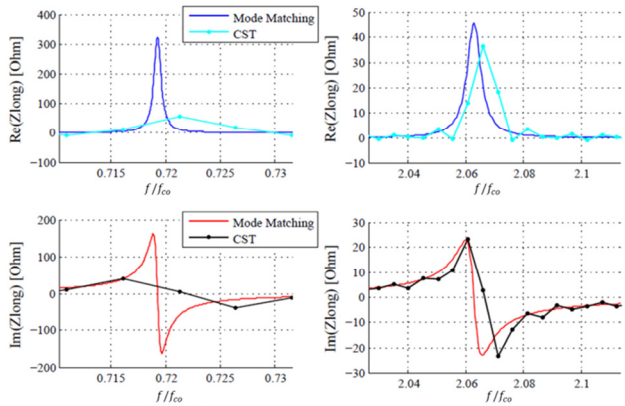

Figure 5: Comparison with CST simulations: b=5cm, c=9cm, L=800um. Material: ε_{dr}=9.9, μ_{dr}=1, σ=10^{-2} S/m.

Below cut-off, since the dielectric losses are very low, the Q is very high; above cut-off (right plot) the peaks are lower due to the leak into the beam pipe. The correct estimation of the Q factor is very important since these resonances could lead to coupled bunch instabilities.

CONCLUSION

The longitudinal beam coupling impedance of a finite length device was successfully derived and benchmarked with existing theory and numerical simulations for the longitudinal component of the beam coupling impedance in the non ultrarelativistic case.

Considering the real finite length of a device is important both for high conductivity materials, and for low conductivity ones: in the first case the impedance above cut-off have to include the contribution of the beam pipes; in the second case the resonances depend on the length of the device and the losses in the material, this could lead to beam coupling instability if these modes are not properly damped (lowering the Q factor).

Further extension to the driving (dipolar) and detuning (quadrupolar) impedances is under development.

REFERENCES

[1] R.L Gluckstern, B.Zotter, "Longitudinal Impedance of a Resistive Tube of Finite Length", CERN unpublished.
[2] Y. Shobuda, Y.H. Chin, K. Takata "Coupling impedances of a resistive insert in a vacuum chamber", PhysRevSTAB, 2009.
[3] G. Stupakov, " Resistive wall impedance of an insert", SLAC-PUB-11052 – 2005.
[4] G. Franceschetti, "Electromagnetics: Theory, Techniques, and Engineering Paradigms " Springer-Verlag New York, June 1997.
[5] J. G. Van Bladel, "Electromagnetic Fields",(IEEE Press Series on Electromagnetic Wave Theory, 2007.
[6] CST Computer Simulation Technology AG.
[7] L. Palumbo, V.G. Vaccaro, M. Zobov, "Wake Fields and Impedance", CAS school 1994.

ISBN 978-3-95450-115-1